Evaluation of the Dynamic Deformable Elastic Template model for the segmentation of the heart in MRI sequences

Christopher Casta[1], Patrick Clarysse[1], Joël Schaerer[1] and Jérôme Pousin[2]

[1] Université de Lyon, CREATIS; CNRS UMR5220; INSERM U630; INSA-Lyon;
[2] Université de Lyon, ICJ; CNRS UMR5208; INSA-Lyon;
Université Lyon 1; 69621 Villeurbanne, France.

Abstract. We introduce a bio-inspired dynamic deformable (DET) model based on the equation of dynamics and including temporal smoothness constraints. The behaviour and characteristics of the dynamic DET model is studied in the context of the semi automatic spatio-temporal segmentation of the left ventricle myocardium in cine-MR images. The segmentation accuracy for endo/epicardium contours at end-diastole and end-systole, and as consequence the performance and limits of the current implementation, is evaluated in the context of the MICCAI LV Segmentation Challenge on a database of 15 multi-slice cine-MRI examinations.

1 Introduction

The detailed analysis of cardiac images remains a challenging task. In particular, the automated analysis of cardiac anatomical and functional Magnetic Resonance (MR) images could yield detailed anatomical and functional cardiac parameters such as 3D shapes and volumes, motion, strains and stresses in the myocardium.

In this paper, we present a new approach for the segmentation and motion tracking of the myocardium in dynamic MRI sequences. Our method is based on the *Deformable Elastic Template* (DET) method introduced by Pham [1], and later improved by Rouchdy [2]. A *Deformable Elastic Template* is a combination of :

- A topological and geometrical model of the object to be segmented (here, the heart muscle).
- A constitutive equation (elasticity) defining its behavior under applied external image forces that push the model's interfaces towards the image edges.

Here, we extend this approach to the temporal dimension, in order to fully take into account the dynamics of the heart over the cardiac cycle. The proposed approach, named *DynamicDET*, imposes temporal smoothness and periodicity constraints to the model, thus improving the robustness. It also analyzes all time frames concurrently, contrarily to most other approaches which analyze only one

instant at a time. The performance of DynamicDET is assessed in the context of the MICCAI 2009 LV Segmentation Challenge :
`http://smial.sri.utoronto.ca/LV_Challenge/Home.html`

2 Dynamic DET model description

2.1 Static DET model

The dynamic DET model is an extension of the previously introduced static DET model [1].

The DET model is a deformable volumetric model submitted to external constraints imposed by the image. The equilibrium of the model is obtained through the minimization of the following global energy functional :

$$E = E_{elastic} + E_{data}$$

where $E_{elastic}$ represents the elastic deformation energy of the model and E_{data} is the energy due to the external image forces f, which are respectively given by:

$$E_{elastic} = \frac{1}{2}\int_{\Omega} \mathrm{tr}(\sigma\epsilon^T)\, d\Omega, E_{data}(u) = -\int_{\partial\Omega} f(u)\, d\gamma$$

where σ and ϵ are the 3D strain and deformation tensors and Ω is the model domain at rest. The material is considered to be isotropic, homogenous and completely defined by its Young modulus and its Poisson coefficient. $\partial\Omega$ is the border of the object domain Ω.

These energy terms can be approximated by discretizing the displacement u and the force f, using the finite element method (FEM). The displacement is approximated by linear functions on these elements, while the forces are sampled at nodal points. Under this approximation, the minimum of the energy must satisfy the following equation:

$$\mathbf{KU} = \mathbf{F}(\mathbf{U}) \tag{1}$$

where $\mathbf{K}$ is the stiffness matrix, corresponding to the response of the elastic material, and $\mathbf{U}$ and $\mathbf{F}$ are respectively the displacement and the force vectors on mesh nodes. To solve this equation, we construct an evolution equation that allows to solve the nonlinear problem by solving a series of linear systems:

$$\frac{d\mathbf{U}}{d\tau} + \mathbf{KU} = \mathbf{F}(\mathbf{U})$$

where τ is the evolution parameter.

The model resulting from equation 1 is purely static. In the next section, we extend the method to the analysis of dynamic image sequences by considering the equation of dynamics in place of equation 1.

2.2 Dynamical DET model

Image data We assume the data is available as sequences of N 2D or 3D images, sampling the cardiac cycle. To simplify the mathematical treatment of the problem, we assume that the cardiac cycle is parameterized by $t \in [0, 1[$.

Simplified equation of dynamics In this work, the heart dynamic is controlled by the simplified dynamics equation (where acceleration is neglected):

$$\mathbf{D}\dot{\mathbf{U}} + \mathbf{K}\mathbf{U} = \mathbf{F}(\mathbf{U}, t) \tag{2}$$

We consider the matrix $\mathbf{D}$ to be a multiple of identity. It can thus be replaced by a single scalar α.

Function basis Our goal is to match a geometrical heart template to a moving sequence of images, while satisfying periodicity and smoothness of the motion. In order to enforce these constraints, we look for solutions in a finite-dimension subspace $\mathcal{F}$ generated by a set of Fourier harmonics [3].

The frames represent a collection of uniformly-spaced noisy samples of a smooth and periodic phenomenon. Thus, we can assume the force fields $\mathbf{F}^n$ derived from the images to be samples of an element of $\mathcal{F}$. One and only one element of $\mathcal{F}$ satisfies $\mathbf{F}(\frac{n}{N}) = \mathbf{F}^n$, $\forall n, 0 \leq n < N$. The discrete Fourier Transform of the $\mathbf{F}^n$ samples is defined as:

$$\mathbf{dft}[l] = \frac{1}{N} \sum_{n=0}^{N-1} \mathbf{F}^n e^{\frac{-2\pi i l n}{N}}$$

and

$$\mathbf{f}^l = \begin{cases} \mathbf{dft}[l], & \forall l,\ 0 \leq l < \frac{N}{2} \\ \mathbf{dft}[l+N], & \forall l,\ -\frac{N}{2} < l < 0 \\ \frac{1}{2}\mathbf{dft}[\frac{N}{2}], & \forall l,\ l = \pm\frac{N}{2} \end{cases}$$

then

$$\mathbf{F}(t) = \sum_{l=-N/2}^{N/2} \mathbf{f}^l e^{2\pi i l t}$$

Note that the previous expressions are only valid if N is even. Similar expressions can be easily derived for the odd case.

In order to reduce the noise impact and to enforce smoothness of the motion, either data or the computed solution are filtered out. In the Fourier basis, filtering the high frequencies can be as easy as removing the high frequency harmonics, more precisely, setting $\mathbf{f}^l = \mathbf{f}^{-l} = 0$ for $l > a$, where a is the highest admissible frequency. Note that filtering $\mathbf{F}$ before solving the equation is equivalent as filtering $\mathbf{U}$ *a posteriori*, as can be clearly seen from the previous mathematical developments.

2.3 Algorithm implementation

Solution to equation (2) is achieved through a pseudo-instationnary process [4]. Roughly speaking, it consists in introducing a parameter τ, and to consider a pseudo-instationnary problem with respect to τ derived from the original problem. Define $\mathbf{AU} = \dot{\mathbf{U}} + \mathbf{KU}$ and consider,

$$\begin{cases} \frac{d\mathbf{U}}{d\tau} & = \mathbf{F}(\mathbf{U}) - \mathbf{AU} \\ \mathbf{U}(0) = 0. \end{cases} \tag{3}$$

if $\mathbf{U}$ converges when $\tau \rightarrow +\infty$, then it tends towards a limit which is a solution of the nonlinear time dependent problem. Discretizing the previous equation with finite differences to solve the temporal equation leads to:

$$(\frac{1}{\Delta\tau} + \mathbf{A})\mathbf{U}^{\tau} = \mathbf{F}(\mathbf{U}^{\tau-1}) + \frac{1}{\Delta\tau}\mathbf{U}^{\tau-1}$$

$$(\frac{1}{\Delta\tau} + \frac{\alpha}{\Delta n} + \mathbf{K})\mathbf{U}_n^{\tau} = \mathbf{F}(\mathbf{U}_n^{\tau-1}) + \frac{1}{\Delta\tau}\mathbf{U}_n^{\tau-1} + \frac{\alpha}{\Delta n}\mathbf{U}_{n-1}^{\tau}$$

which is a linear system and is thus straightforward to solve.

3 Method parameters and User Interaction

The parameters of the algorithms can be divided into the following categories :

- **Initial Template:** In 2D spatial dimension, the initial template consists in a ring representing both endocardium and epicardium. It is defined with three geometrical parameters: the center of the annulus, the radius and the thickness. These parameters are manually defined by the user on the ED frame, in order to ensure a good positioning of the template at the beginning of the algorithm. The template is meshed by dividing the ring into triangles from a regular partition of the LV into sectors and concentric rings (see Figure 1). The number of rings and sectors are two other parameters defining the mesh.
- **Mechanical parameters:** The Young modulus represents the rigidity of the model, while the Poisson coefficient characterizes the ability of the material to be compressed.
- **Algorithm parameters:** The stopping criteria defines when the algorithm has converged. We can also choose the number of resolution levels with which the sequence images are processed.

We mainly act on two parameters which are the Young modulus and the resolution level number. If the Young modulus is set too high, the model will not deform at all. If set too low, the model will deform to match all image features, real structures and artifacts alike. Concerning the resolution level number, using a single level works correctly if the magnitude of the deformation is not too important. However, if there is a large movement or thickening throughout the dynamic sequence, it may be necessary to use several resolution levels to allow larger deformations.

4 Results

We present the results obtained on the validation set used for the MICCAI Challenge. The validation set consists of 15 examinations with 4 patient categories (heart failure, with (HF-I) or without (HF-NI) ischemia, hypertrophy (HYP) and normal (N)). Examinations are made of 8 to 14 slice levels. Evaluation is performed only for endocardium and pericardium contours at ED and ES frames. We observe that the segmentation results depend on the actual motion of the heart, ie. the pathology affecting the patient's heart.

Figure 1 shows the results of a LV segmentation on a patient affected by heart failure with ischemia (Slices 41 to 60 of the HF-I-05 dataset), with Mean=2.1986mm and Std=1.0643mm for systole and Mean=2.3859mm and Std=1.9907mm for diastole, both for inner contours. Figure 2 shows the result of a segmentation on a normal patient (Slices 88 and 99 of the N-06 dataset), with large thickening, with Mean=6.179mm and Std=4.4329mm for systole and Mean=2.576mm and Std=1.531mm for diastole, both for inner contours.

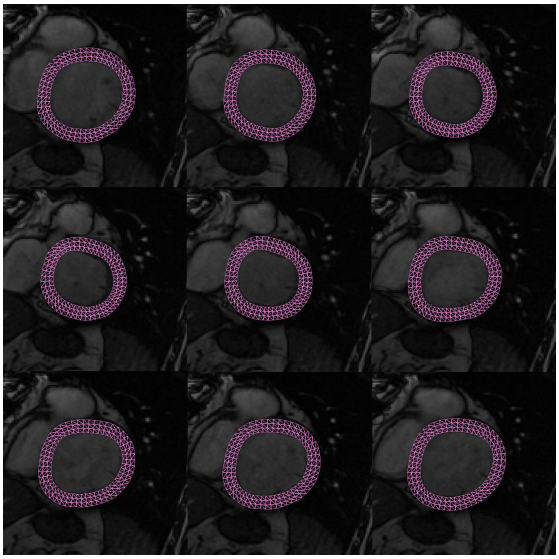

Fig. 1. DET Model superimposed onto the images of HF-NI-05 sequence at a median slice of the heart over the cardiac cycle. The sequence should be read like a book, with end-diastole on the top-left corner (only one over two frames are shown). The pink mesh is the model. It is set to be translucent so that correspondence between model and image contours can be appreciated.

Table 1 presents the left ventricle mass (LVM) for a selection of patients, for both automatic and manual segmentations. Volume Ratio (VR), defined as the ratio of expert and estimated LVM, was calculated to estimate the quality

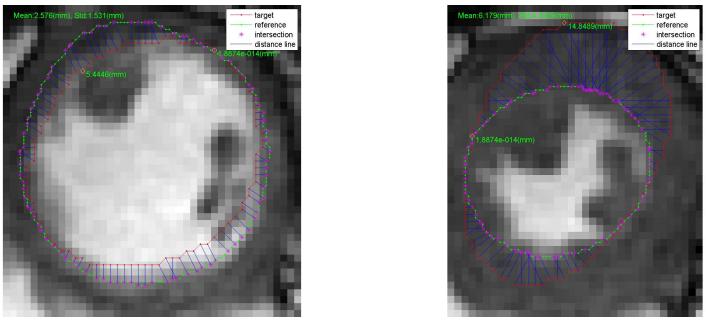

(a) (b)

Fig. 2. Segmentation problems with thickening : (a) Correct segmentation at end-diastole, (b) Difficulties when following the course of the endocardium up to the end-systole. The green contour is the reference, the red contour is our segmentation.

of the results. Table 2 references average values and standard deviation for VR over the left ventricle mass for the different pathology classes. Table 3 presents the ejection fraction (EF) for different datasets, for both automatic and manual segmentations. The relative error was calculated to estimate the quality of the results.

Patient ID	Auto LVM	Manual LVM	Volume Ratio
HF-I-06	151.4182	153.5477	0.9861
HF-NI-07	133.7539	130.5429	1.0246
HYP-07	112.7256	143.4020	0.7861
N-07	68.5166	113.5720	0.6033

Table 1. Left Ventricule Mass (LVM) and therefore Volume Ratio (VR) result depends on the pathology the patient is affected by. HF-I: heart failure with ischemia, HF-NI: heart failure without ischemia, HYP: hypertrophy, N: normal. Ideal volume ratio should tend towards 1.

5 Discussion and Conclusion

The main advantage of our method is that it allows the segmentation of both endo/epicardium of a whole dynamic sequence of images, once the template initialization is done. However, the present evaluation only considers the ED and ES frames. It can accurately follow the deformations of the LV when thickening

Patient ID	$\bar{VR}$	σ
HF-I-*	1.0197	0.0052
HF-NI-*	0.7933	0.1106
HYP-*	0.5717	0.0505
N-*	0.7502	0.0620

Table 2. Average Volume Ratio $\bar{VR}$ and Standard Deviation σ for each patient data class.

Patient ID	Auto EF	Manual EF	Relative Error
HF-I-05	16.9460	30.3025	0.4408
HF-NI-07	3.3729	12.9111	0.7388
HF-NI-33	42.2330	55.2309	0.2353
N-05	35.9429	60.6372	0.4072

Table 3. Ejection Fraction (EF) for several datasets, results with our automated method and with the manual expert one.

is moderate. The interactive initialization of the template is usually fast, but can be delicate in some cases. The computational time of the LV segmentation in the whole sequence was around 0.5 minute on average.

Whatever the image set, the algorithm gets accurate results for outer contours. Each of the segmentations for outer contours is under the average distance threshold of 5mm, ensuring a "good" result in the sense of the contest, with an average distance of $2.7269mm$ and a Dice metric of 0.9272 over the 15 datasets.

However, the method has difficulties getting accurate results when the course of the endocardium is very fast and when thickening is important. The inherent rigidity of our model prevents too large thickening. Setting Young's modulus to a low value allows thickening, but the model will then deform to match image details, which is not suited either. As the template is initialized at the end-diastole phase, segmentation for the diastole is generally correct, but due to thickening, current implementation of the method cannot always follow the course of the endocardium during the systolic phase.

As a result, the LVM is accurate for datasets where thickening is moderate, but is underestimated when larger thickening occurs. Therefore, we observed that the accuracy of the results varies upon the pathology class as shown in Table 1. LVM ratio is always over 0.85 for patients affected by heart failure with ischemia, due to a reduced thickening during a cardiac cycle. Concerning the other cases, which all involve thickening, the computed volume ratio greatly fluctuates (from 0.2027 in the worst case to 1.1960) and can take values far from the ground truth (Table 2).

As a consequence, this lack of thickening capacity sometimes leads to inaccurate results concerning the calculation of the ejection fraction (EF). While the expert segmentation has EF going from 12.9111% to 68.7816%, our results only go up to 42.2330%, and are generally underestimated. Some results are compiled in Table 3. This is problematic in the sense that the EF is one of the most

important functional parameters with clinical value. To tackle this problem, we currently investigate various approaches. One consists in attributing to the LV endocardium a specific rigidity with a Young modulus higher than the inside LV. Another solution is to refine the edge map which attracts the DET model based on a prior segmentation (e.g. a 2D+t morphological segmentation) and selective application of forces.

As a conclusion, we presented our dynamic DET model for heart segmentation and tracking in cine-MRI. Its great advantage is that it performs simultaneously the segmentation of both endo/epicardium over the whole image sequence and is able to provide strain maps as well. User input is reduced: placement of the initial template in the ED frame and settings of the Young modulus and resolution level number. The evaluation through the MICCAI Challenge database allowed us to assess more largely the performance of dynamic DET for the LV segmentation and its main advantages and limits. We are currently working on the 4D version of dynamic DET, which would require 4D evaluation as well. This is actually the objective our French initiative IMPEIC of GDR STIC-Santé (`http://stic-sante.org/`) for segmentation and evaluation in cardiac imaging.

6 Acknowledgements

This work is supported by the French ANR GWENDIA under contract number ANR-06-MDCA-009. The Région Rhônes-Alpes is gratefully acknowledged for its support through the project Simed of the cluster ISLE as well as the CNRS-GDR STIC-Santé through the support of the IMPEIC action.

References

1. Q. PHAM, F. VINCENT, P. CLARYSSE, P. CROISILLE and I. MAGNIN, "A FEM-based deformable model for the 3D segmentation and tracking of the heart in cardiac MRI",*in Proceedings of ISPA 2001*,p. 250-254, 2001.
2. Y. ROUCHDY, J. POUSIN, J. SCHAERER and P. CLARYSSE, "A nonlinear elastic deformable template for soft structure segmentation : application to the heart segmentation in MRI",*Inverse Problems*, vol. 23,p. 1017-1035, 2007
3. A. V. OPPENHEIM, R. W. SCHAFER and J. R. BUCK, *Discrete-time signal processing (2nd ed.)*. Upper Saddle River, NJ, USA : Prentice-Hall, Inc., 1999.
4. P. G. CIARLET and J.-L. LIONS, *Handbook of Numerical Analysis, Volume 1, Finite difference methods, Solution of equations in* Z^n.$North - Holland$, 1990.
5. J. SCHAERER, J. POUSIN, P. CLARYSSE. "A new singular perturbation approach for image segmentation tracking", *in Biomedical Imaging: From Nano to Macro. ISBI 2008. 5th IEEE International Symposium on*, p. 1445-1448, May 2008.
6. J. SCHAERER, P. CLARYSSE, Y. ROUCHDY and J. POUSIN, "A dynamic elastic model for heart segmentation and motion estimation", *Medical Image Analysis*, in revision.
7. P. RADAU, Y. LU, K. CONNELLY, G. PAUL, A.J. DICK, G.A. WRIGHT. "Evaluation Framework for Algorithms Segmenting Short Axis Cardiac MRI.", *The MIDAS Journal - Cardiac MR Left Ventricle Segmentation Challenge*, `http://hdl.handle.net/10380/3070`